

STRUCTURAL, DYNAMICAL & ELECTRONIC PROPERTIES OF CaCuO_2

by

Bal K. Agrawal and Savitri Agrawal

Physics Department, Allahabad University,
Allahabad 211002, INDIA.

The scalar relativistic version of an accurate first principles full potential self-consistent linearized muffin tin orbital (LMTO) method has been employed for describing the physical properties of the parent system of the high T_c oxide superconductors, i.e., CaCuO_2 . The presently employed modified version of the LMTO method is quite fast and goes beyond the usual LMTO-ASA method in the sense that it permits a completely general shape of the potential and the charge density. Also, in contrast to LMTO-ASA, the present method is also capable of treating distorted lattice structures accurately. The calculated values of the lattice parameters of pure CaCuO_2 lie within 3% of the experimentally measured values for the Sr-doped system $\text{Ca}(.86)\text{Sr}(.14)\text{CuO}_2$. The computed electronic structures and the density of states is quite similar to those of the other oxide superconductors, except of their three-dimensional character because of the presence of strong coupling between the closely spaced CuO_2 layers. The van Hove singularity peak appears slightly below the Fermi level and a small concentration of oxygenation /or/ substitutional doping may pin it at the Fermi level. The calculated frequencies for some symmetric frozen phonons for undoped CaCuO_2 are quite near to the measured data for the Sr-doped CaCuO_2 .

I. INTRODUCTION

The present LMTO method is seen to produce the electronic structure, cohesive energy, lattice constants, elastic constants, phonon frequencies, mode Grüneisen and strain parameters for the simple systems like Si, C etc [1]. Very recently, the method has been successfully applied also for the III-V and II-VI semiconducting compounds like AlAs, CdTe, GaSb, ZnSe, ZnTe, ZnS etc [2,3]. The influence of structural relaxation of the atoms on the valence-band off-set at the lattice matched

interfaces of II-VI and III-V semiconductors ZnTe/GaSb(110) and the lattice mismatched interface ZnS/ZnSe(001) has been investigated [4]. Very recently the van Hove singularity scenario and hole concentrations at different pressures for the Hg-based oxide superconductors have been investigated [5].

A compound CaCuO_2 is obtained if the number of CuO_2 planes is allowed to increase indefinitely ($n \rightarrow \infty$). Thus, CaCuO_2 is the infinite number of CuO_2 layers limit of the above superconductors and is seen to be insulating [6]. T_c might increase with n . The $n = \infty$ material appears to be more difficult to dope. However, more recently $(\text{CaSr})\text{CuO}_2$ has been doped successfully and an electron type superconductivity has been seen [7]. In practice, the $n = \infty$ structure is not formed with only Ca ion on A site, a material with some Ca substitution by Sr, $\text{Ca}(0.86)\text{Sr}(0.14)\text{CuO}(2)$ has been prepared. The Sr-mixed compound is seen to be narrow band semiconductor. For details of the LMT0 method we refer to the earlier papers [1-4].

II. CALCULATION AND RESULTS

The CaCuO_2 structure as shown in Fig.1 has a space group $P4/mmm$ (D_{4h}). The atomic positions in the unit cell are $\text{Cu}:(0,0,0)$; $\text{O}(1):(.5a,0,0)$; $\text{O}(2):(0,.5a,0)$; $\text{Ca}:(.5a,.5a,.5c)$.

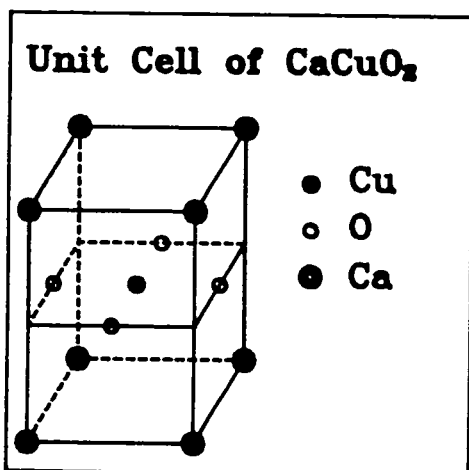


FIG.1 Unit cell for the crystal structure of CaCuO_2 .

For the Sr-doped sample the experimental lattice parameters are $a=3.86 \text{ \AA}$ and $c=3.2 \text{ \AA}$. The bond lengths are $\text{Cu-O}(1) = \text{Cu-O}(2) = 1.93 \text{ \AA}$ and $\text{Ca-O}(1) = \text{Ca-O}(2) = 2.50 \text{ \AA}$.

In the present calculation, the basis employed for making expansions of the products of the LMT0 envelops included functions with $l \leq 4$ and of energies -0.01 , -1.0 and -2.3 Rydberg and with decays given by $\lambda_2 = -1$ and -3 Rydberg. The set will include 50 functions

for each atomic sphere. The local density potential of Hedin and Lundquist has been employed. An absolute convergence to better than 1.5 mRy/atom is obtained with spd basis of 22 LMTO's/atom for each atom including O. The number of atoms in unit cell were taken to be four.

The muffin tin (MT) spheres were chosen to be slightly smaller than touching and the radii for Cu, O and Ca were taken as 1.88, 1.64 and 2.99 atomic units(a.u.), respectively. The states Cu(3d,4s,4p), O(2s,2p) and Ca(3p,3d,4s) are taken as the valence band electrons. An empty sphere has been included at (0,0,.5c) in the calculation.

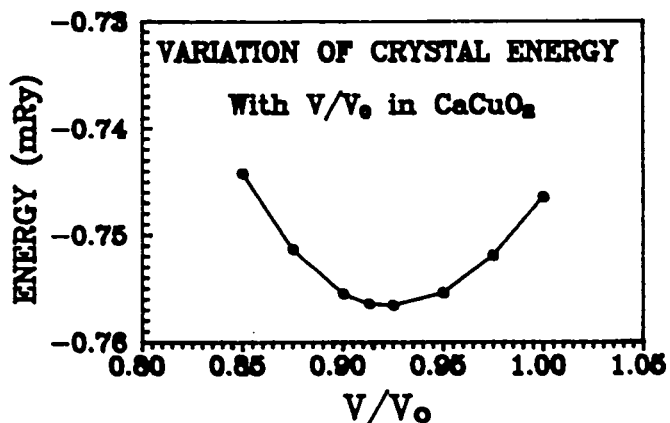


FIG.2 Variation of crystal energy (mRy) with the ratio of unit cell volumes, V_0 and V as described in the text.

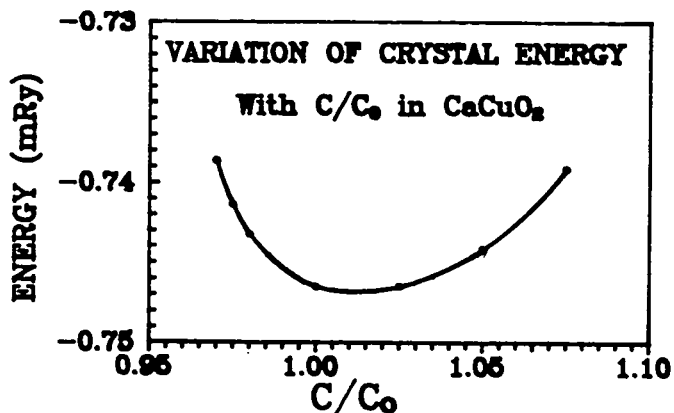


FIG.3 Energy variation with the interplaner spacing.

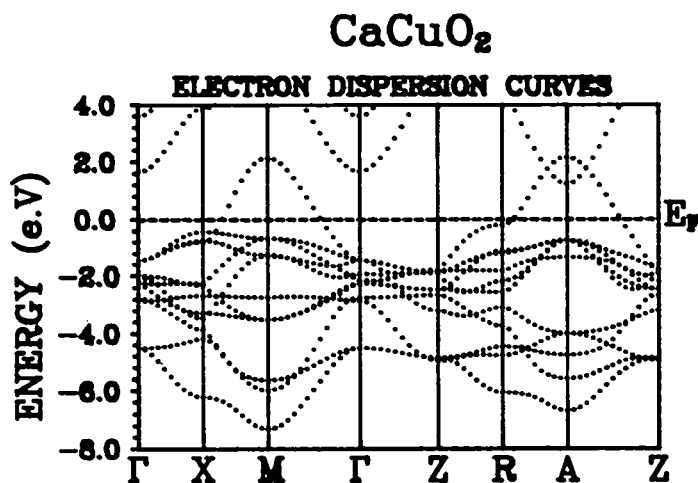
Variations both in the lattice parameter 'a' and the ratio c/a were investigated. The results are shown in Figs. 2 & 3, respectively. One finds energy minimum for a volume of the unit cell $V = 0.925 V_0$ and $c/a = 1.00$, where V_0 is the unit cell volume for $a = 3.86 \text{ \AA}$ (in fact, these lattice parameters correspond to the experimental values for the Sr doped CaCuO_2). So the values of a and c are quite close to those for Sr-doped material. The

calculated value of 'c' is within 3% of the experimental value. The calculated value of bulk modulus is 1.99 Mbar.

The charge transfer from the muffin tin spheres (i.e., the difference between the atomic number and charge lying within the MT sphere) of Cu, O and Ca are 1.65, 0.56, and 0.62 electron charges, respectively. The total electron charge per unit cell outside the MT spheres is 3.39e.

(A) ELECTRONIC STRUCTURE

The calculated band structure along some symmetry directions is presented in Fig. 4. The various symmetry points of the Brillouin zone in units of $2\pi/a$ are $\Gamma(0,0,0)$; $X(.5,0,0)$; $M(.5,.5,.6)$; $Z(0,0,.6)$; $R(.5,0,.6)$ and $A(.5,.5,.6)$. As the spacing between the two successive CuO_2 layers is smaller than the intraplaner Cu-O separation within the



CuO_2 , the bands along the c-direction show appreciable dispersion although smaller than the dispersion seen within the x-y plane (or Cu-O_2 layer). The Fermi level is set at origin of energy.

FIG.4 Dispersion curves for the CaCuO_2 system.

The lowest 11 bands lying in the energy interval range of about 9 eV near and below Fermi level arise mainly from the $\text{Cu}(3d)$ and $\text{O}(2p)$ states. This spread (≈ 9 eV) of energy bands is similar to that calculated by Mattheiss and Hamann [8] and by Singh et al [9] using LAPW method and by Korotin and Anisimov [10] using the LMTO-ASA method. The uppermost band crossing the Fermi level corresponds to the anti-bonding $\text{Cu-d}[x^2-y^2]:\text{O-p}[x,y]$ states. The lower parts of the $\text{Ca}(3d)$ bands lying above Fermi level overlap the antibonding

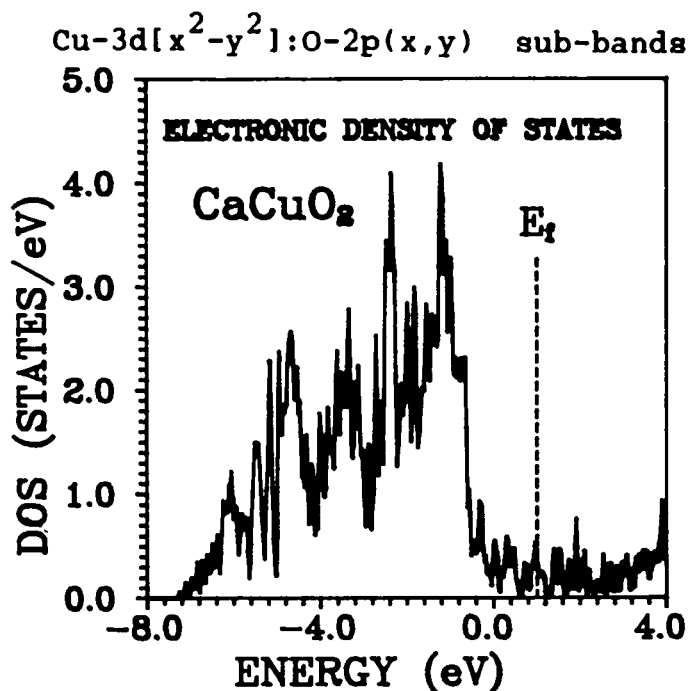


FIG.5 Total electronic DOS.

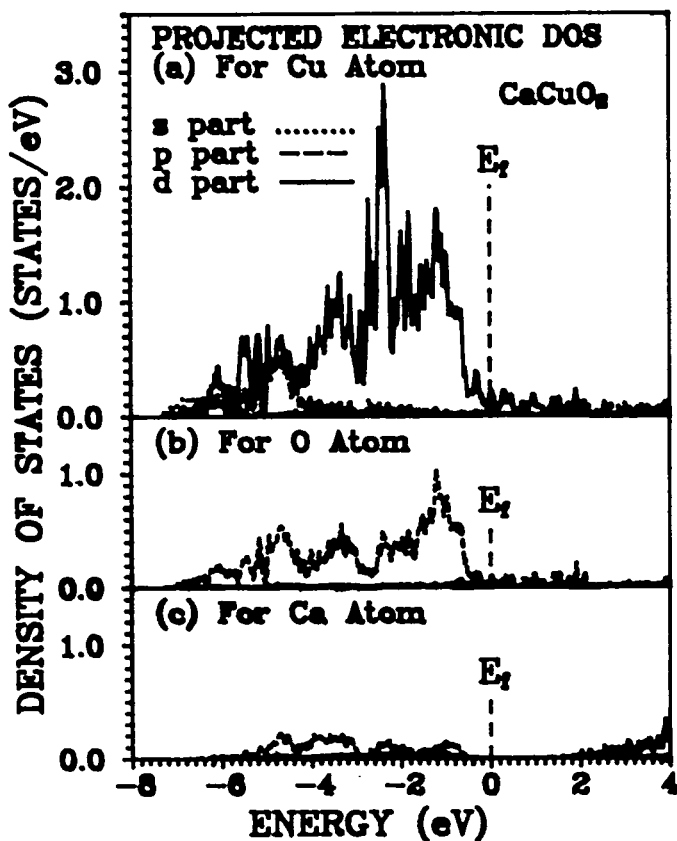


FIG.6 Projected DOS for Cu, O and Ca atoms with s, p & d orbitals contribution.

near Γ and A symmetric points.

In order to see the nature of the dispersion in another plane shifted in the c - direction, we have also included in Fig. 4 the dispersion curves in the $2\pi/a[0,0,0.6]$ direction. There appear saddle points at -0.81 eV at X point and at -0.19 eV at R point.

In the calculation of the total density of states (DOS), a sampling method for 196 k points in the irreducible part of the Brillouin zone with a Gaussian energy broadening of 0.002 Ry was employed. The calculated DOS for the self-consistent calculation is shown in Fig. 5. The DOS shows the main features which are quite similar to those of the other oxide high-Tc cuprates. The projected densities at various atoms have also been shown in Fig. 6. At Fermi level, the main contributions arise from Cu(3d) and O(2p) states.

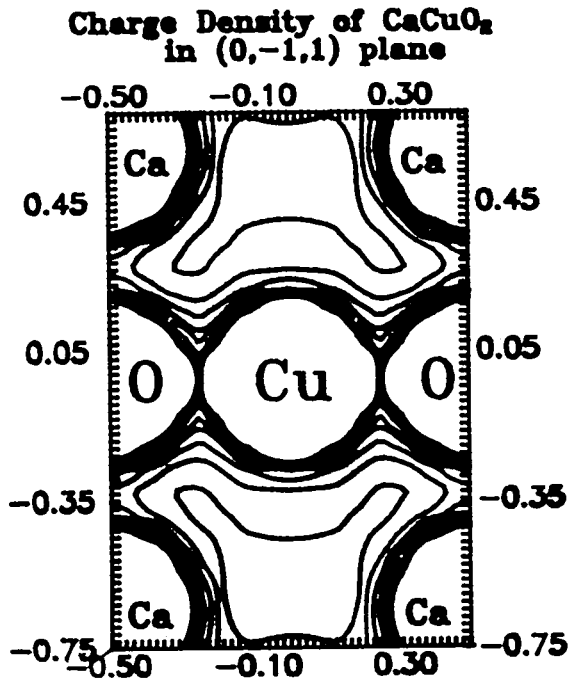


FIG.8 Valence charge density contours in the $(0,-1,1)$ plane in interval of $0.015 \text{ e}/(\text{a.u.})^3$ up to a maximum value of $0.12 \text{ e}/(\text{a.u.})^3$.

remaining sixth mode comprising of the out of (CuO_2) plane vibrations of oxygen atoms in opposite direction is silent. The frequencies of these vibrations alongwith their eigenvectors are presented in Table I. The frequencies have been calculated by determining the harmonic force constant after fitting the energies of the distorted structure for several amplitudes with a polynomial containing terms up to third degree. In order to see the reliability of the estimates of these calculated values we have also included in the table the measured values for the Sr-doped CaCuO_2 . The frequencies for undoped sample are quite close to the observed values for the Sr-doped sample except for Eu mode which involves the motion of all the atoms.

The high degree of the nesting of the Fermi surface is likely to give rise to singularities in the generalized k -dependent electronic susceptibility of the two-dimensional system and may result in the electronically-driven instabilities such as the incommensurate charge or spin density waves.

B. PHONON FREQUENCIES

The variation of the internal energy of the solid with the various types of static deformations in the small displacement limit has been employed for calculating the frozen phonon frequencies at the $\Gamma(k=0)$ point of the Brillouin zone. In CaCuO_2 in all, there are six optical modes out of which five are infrared active and the

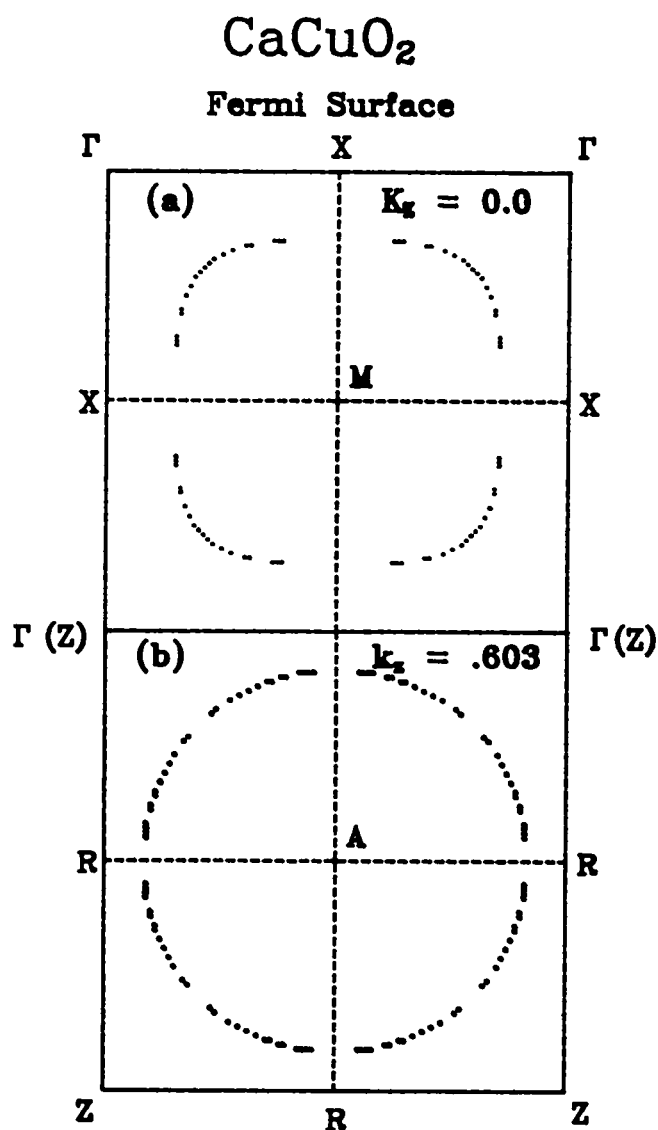


FIG.9 Cross-sections of the Fermi surface in the extended Brillouin zone scheme in two planes (a) $k_z = 0.0$ and (b) $k_z = 0.603$ for CaCuO₂.

III. CONCLUSIONS :

The LMTO method which is comparatively simple and faster than the LAPW method is able to predict one electron energy spectrum of CaCuO₂ quite well. Values for the bulk modulus and the frozen phonon frequencies have been obtained. The phonon frequencies for the undoped CaCuO₂ are quite near to those measured for the Sr-doped sample

TABLE I. Frequencies of the various phonon modes for CaCuO_2 in cm^{-1} .

S. No.	Mode Symmetry	Displaced Atoms	Components of atomic displacements	Calculated freq. for CaCuO_2	Exptl. freq. for Sr-doped CaCuO_2
1.	Au	Cu, Ca	$Z_1 - Z_2$	213	186
2.	Au	O	$Z_3 - Z_4$	316	
3.	Au	Cu, O, Ca	$\begin{pmatrix} Z_1 - Z_2 \\ -Z_3 \\ -Z_4 \end{pmatrix}$	422	421 (440)
4.	Eu	Cu, Ca	$\begin{pmatrix} X_1 - Y_1 \\ -X_2 + Y_2 \end{pmatrix}$	323	230 (240)
5.	Eu	Cu, O, Ca	$\begin{pmatrix} -X_1 - Y_1 \\ -X_2 - Y_2 \\ +Y_3 - X_4 \end{pmatrix}$		306 (40)
6.	Eu	Cu, O	$\begin{pmatrix} -X_1 - Y_1 \\ +X_3 - Y_4 \end{pmatrix}$	634	597 (663)

The displacements of the various atoms are denoted by $\text{Cu}(X_1, Y_1, Z_1)$, $\text{Ca}(X_2, Y_2, Z_2)$, $\text{O}_1(X_3, Y_3, Z_3)$ and $\text{O}_2(X_4, Y_4, Z_4)$.

ACKNOWLEDGEMENTS

The financial assistance from University Grants Commission, New Delhi and Department of Science and Technology, New Delhi are acknowledged.

REFERENCES

1. M. Methfessel, Phys. Rev., B38, 1557 (1988); M. Methfessel C.O. Rodriguez and O.K. Anderson Phys. Rev., B40, 2009 (1989).
2. Bal K. Agrawal and Savitri Agrawal, Phys. Rev., B45, 8321 (1992).
3. Bal K. Agrawal, Savitri Agrawal and P.S. Yadav, preprint (1994).
4. M. Methfessel, Bal K. Agrawal & M. Scheffler, Proc. Int. Conf. of Physics of Semiconductors, 1990, Greece; Bal K. Agrawal and Savitri Agrawal, preprint, (1994).
5. Bal K. Agrawal and Savitri Agrawal, Physica C, (1994) in press; High Tc update, 1 May, (1994).
6. T. Siegrist, S.M. Zahurk, D.W. Murphy, & R.S. Roth, Nature 334, 193 (1988).
7. X. Smith et al., Nature 351, 549 (1991).
8. L.F. Mattheiss and D.R. Hamann, Phys. Rev. B40 2717 (1989).
9. D. Singh, W.E. Pickett and H. Krakacur, Physica C, 162-164, 1431 (1989).
10. M.A. Korotin and V.I. Aniscimov, Mater. Lett. 10, 28 (1990).
11. G. Burns et al, Phys. Rev. B40, 6717 (1989).